

## Solar energy model and thermal performance of an electrochromic dome-covered house



Yaolin Lin <sup>a,b,\*</sup>, Wei Yang <sup>c</sup>

<sup>a</sup> School of Civil Engineering and Architecture, Wuhan University of Technology, Wuhan, Hubei 430070, PR China

<sup>b</sup> Centre for Building Studies, Department of Building, Civil and Environmental Engineering, Faculty of Engineering and Computer Science, Concordia University, 1455 Maisonnette W., Montreal, Quebec H3G1M8, Canada

<sup>c</sup> College of Engineering and Science, Victoria University, Melbourne 8001, Australia

### ARTICLE INFO

#### Article history:

Received 4 July 2016

Revised 22 October 2016

Accepted 1 May 2017

Available online xxxx

#### Keywords:

Solar energy model

Thermal performance

Dome-covered house

Sustainable development

Electrochromic glazing

### ABSTRACT

A dome-covered house can be considered as a sustainable building design example. It mimicks the optimal forms in the nature, and can help achieve reduction on the house heating energy need in cold winter. When the dome is made of electrochromic glazing, it can prevent large amount of solar energy from passing into the interior of the dome to prevent over-heating in summer. In this paper, a three-dimensional solar energy, thermal and air flow model is presented. The impact of different glazing types on the thermal environment inside the dome in summer and house heating load in winter is investigated. The use of electrochromic/low transmissivity glazing can result in the reduction of the absorption of solar radiation by the ground for up to 88.9%, as compared to the normal glazing and help to reduce the highest air temperature inside the dome from 41.8 °C to as low as 25.6 °C at 1:00 PM on July 21st in Montreal at 45°N latitude, southern part of Canada, and from 34.6 °C to 20.6 °C in Yellowknife at 62.5°N latitude, northern part of Canada, under different control strategies, thus can create a comfortable thermal environment inside the dome.

© 2017 International Energy Initiative. Published by Elsevier Inc. All rights reserved.

### Introduction

While designers are striving to use material and energy more efficiently, it is expected that much of the conventional, modern architectures are not sustainable over the long term due to their lack of consideration on the interaction between buildings and environment. On the other hand, nature itself has undergone billions of years' evolution and can provide lessons to learn, especially on how to build habitats to integrate harmonily with the environments by the creatures (Tsui, 1999). Design by learning from the optimal forms existing in nature is a possible way towards sustainable buildings since they are selected by nature through billions of years' evolution. Dome mimicks form-optimizing process in the nature and may be represented as pneumatic structure in the architectural world (Stach, 2004; Arslan and Sorguc, 2004). The dome configuration utilizes nature's principles to form a highly efficient system. A dome in northern Canada is a shelter to withstand extreme weather condition, and store large amounts of solar radiation to achieve reduction on the heating energy need of the covered house in the winter.

One zone model (Croome and Moseley, 1984; Luttmann-Valencia, 1990; Singh et al., 2006) and four-zone model (Sharma et al., 1999) were developed to predict the air temperature inside such structure, assuming well-mixed air in each zone. The temperature distribution of the cover was not computed and fixed value of the convection coefficient was imposed, and transmitted solar radiation was simplified by those models (Croome and Moseley, 1984; Luttmann-Valencia, 1990; Singh et al., 2006; Sharma et al., 1999).

Some building energy simulation programs, such as eQuest (2016), can calculate the thermal load of the building, but cannot evaluate the airflow and temperature distribution. EnergyPlus (2016) uses certain room air models to account for non-uniform air temperature by dividing a room vertically into several well separated regions and AirflowNetwork model to calculate the air flow through a set of nodes through linkage. TRNSYS (2016) can be coupled with COMIS for multi-zone air flow calculation where each room is represented as a node. Those programs (eQuest, 2016; EnergyPlus, 2016; TRNSYS, 2016), cannot provide detailed air flow and temperature distribution inside an air space. ESP-r (2016) offers the feasibility of detailed air flow simulation and heat transfer prediction inside a room via CFD. However, it will be extremely time-consuming to applied CFD to a large air space for dynamic simulation.

Lin (2007) developed a transient three-dimensional thermal and air flow model of a house built around a large-scale transparent dome. This

\* Corresponding author at: School of Civil Engineering and Architecture, Wuhan University of Technology, Wuhan, Hubei 430070, PR China  
E-mail address: yaolinlin@gmail.com (Y. Lin).

## Nomenclature

A, B, C	solar coefficients;
$A_{ij}$	cell surface area, $m^2$ ;
$A_l$	wall surface area, $m^2$ ;
$C_l$	coefficient;
$C_N$	clearness number;
$c_p$	specific heat of the dome glazing, $J/kg\ ^\circ C$ ;
$d$	thickness of glazing, m;
$f_{h,i}$	hourly usage probability, dimensionless;
$F_{ij,g,out}$	view factor of cell (i,j) to the ground outside, dimensionless;
$F_{ij,l}$	view factor of cell (i,j) to the outside wall surface, dimensionless;
$F_{ij,sky}$	view factor of cell (i,j) to the sky, dimensionless;
$F_{kl,ij}$	view factor of cell (k,l) to cell (i,j), dimensionless;
$F_{l-g}$	view factor of the outside wall surface to the ground inside, dimensionless;
$I_{beam,ij}$	beam solar radiation over cell (i,j), $W/m^2$ ;
$I_{dg,ij}$	incident solar radiation reflected from the outside ground surface to cell (i,j), $W/m^2$ ;
$I_{diff,ij}$	diffuse solar radiation over cell (i,j), $W/m^2$ ;
$I_{ds,ij}$	diffuse incident solar radiation on cell (i,j) from the sky, $W/m^2$ ;
$I_{DN}$	direct normal incident solar radiation on the earth surface, $W/m^2$ ;
$I_{max}$	maximum allowable beam radiation, $W/m^2$ ;
$I_{total,ij}$	total solar radiation on cell (i,j), $W/m^2$ ;
$k$	conductivity of glazing, $W/m\ ^\circ C$ ;
$l_{i+1,j}$	length of the border between cell (i + 1, j) and cell (i, j), m;
$P_{i,j}$	power input to the ith electric appliance in phase j, kW;
$q_{conv,ij}$	convection over cell (i,j), $W/m^2$ ;
$q_{LWR,ij}$	long-wave radiation heat fluxes with the environment (ground and sky), $W/m^2$ ; $q_{sol,ij}$ absorbed incident solar radiation, $W/m^2$ ;
$q_{surf,ij}$	long-wave radiation among cell (i,j) and other surfaces, $W/m^2$ ;
$Q_{HVAC}$	thermal load of HVAC system, W;
$Q_{internal,conv}$	convective internal heat gain, W;
$m_{ij}$	mass of one cell (i,j), kg;
$\dot{m}_{ij}$	mass flow rate, kg/s;
R	radius of the dome, m;
t	time, s;
T	temperature, $^\circ C$ ;
$T_a$	room air temperature, $^\circ C$ ;
$T_j$	temperature of the jth wall/window/roof/floor surface, $^\circ C$ .

### Greek symbols

$\alpha_{ij}$	absorptance of cell (i,j), deg.;
$\alpha_w$	absorptance of outside wall surface, dimensionless;
$\beta$	solar altitude, deg.;
$\rho$	air density, $kg/m^3$ ;
$\gamma_g$	ground reflectance, dimensionless;
$\theta_{ij}$	incident angle over cell (i,j), deg.;
$\tau_j$	time required for phase j, min;
$\tau_{ij}$	transmittance of cell (i,j), dimensionless;
$\varphi$	solar azimuth, deg.

model first discretizes the dome cover into a large number of cells to enable detailed calculation of the first and second transmission of solar radiation and variation of the temperature over the dome cover. Next, the

air space inside the dome is divided into a large number of zones by using the zonal model approach to calculate the distribution of air flow and air temperature. At the same time, the convection coefficients are treated as varied with a number of factors such as wind speed and wind direction.

This model was used to evaluate the impact of the dome glazing on the house heating energy needs but the impact on the thermal environment in summer was not evaluated. In summer, the dome will become a green house and thus the inside air temperature might increase to a level that will not be thermally comfortable. At the same time, the house occupants' behaviors might have an important impact on the thermal load and energy need of the house (Lin et al., 2015). So, how to estimate the thermal load of the house more accurately and create a comfortable thermal environment inside such structure in summer without air-conditioner?

Electrochromic glazing (ECG) may be used to prevent large amount of solar energy from passing into the interior of the dome roof in summer (Porta-Gándara and Gómez-Muñoz, 2005). ECG has certain advantages over conventional glazing, e.g., fully transparent views can be provided (Lee and DiBartolomeo, 2002); when comparing with conventional fixed shading devices, ECG was found to provide the best performance in reducing solar heat gains (Aldawoud, 2013); ECG can effectively reduce discomfort window glare due to highly bright diffuse skylight when solar radiation intensities are high, while providing much of the available daylight and therefore it is not necessarily to increase the need for artificial lighting and there is no sense of obstruction to the outside (Piccolo and Simone, 2009); the average annual daylight glare index (DGI) can be reduced significantly by electrochromic windows with overhangs and significant annual energy use savings was achieved (Lee and Tavit, 2007).

EC windows could reduce total energy use of  $\geq 45\%$ , peak load carbon emission up to 35% in new construction and 50% in renovation projects for different climate condition in USA (Sbar et al., 2012). For a conference room in Washington DC, EC windows with advanced automated control, thermally improved frames, and dimmable lighting system can save 91% in lighting energy, compared to the existing lighting system (Lee et al., 2012). The use of electrochromic wall can result in total heating and cooling energy savings of 17.6% compared to traditional wall, and of 29.5% compared to Trombe wall in Mediterranean climates (Pittaluga, 2013).

This paper aims at investigating the impact of different types of dome glazing on the thermal environment inside such structure in summer as well as on the reduction of heating load of the house in winter. Three different types of glazing, i.e., normal glazing, ECG under different continuous and discrete control strategies, and glazing with low transmissivity, are analyzed. The transient three-dimensional thermal and air flow model is coupled with control strategies of ECG and occupant behaviors model to be able to predict more accurately on the thermal load of the house and the thermal comfort condition inside the dome. The impact of glazing and control strategies on the reduction of heating load in winter as well as variation of inside air temperature in summer and impact on solar radiation absorbed by the ground inside the dome are presented.

## Description and modeling of the problem

### Heat fluxes

A schematic diagram on the heat fluxes of the system is presented in Fig. 1. The involved heat fluxes in this system can be summarized as: 1) solar heat gain to the dome cover, ground and house envelop; 2) long-wave radiation among sky, dome surface, ground and house envelop; 3) convection over dome surface, house envelop and ground; 4) infiltration/ex-filtration through the dome and house; 5) conduction through the dome, ground, floor and envelop of the house.

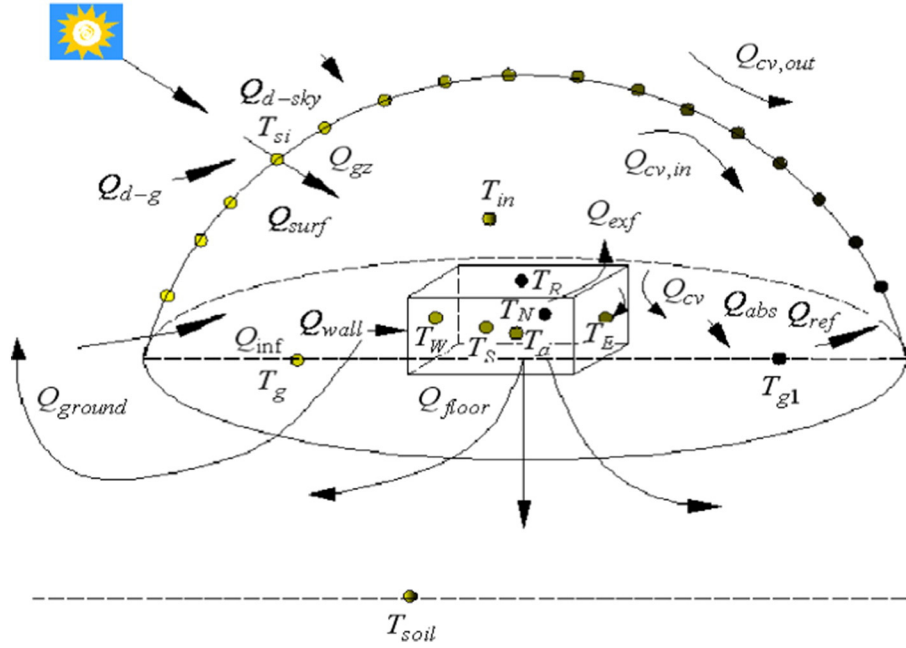


Fig. 1. Heat fluxes of the proposed model.

### Solar radiation

The incident solar radiation includes direct beam solar radiation, first and second transmitted beam solar radiation, diffuse solar radiation, and transmitted diffuse solar radiation.

The beam solar radiation upon the dome is composed of two parts. In one part it receives direct solar beam, and in the other it receives transmitted beam radiation through the other part of the dome.

For the first part, the absorbed solar beam radiation is written as:

$$I_b = \alpha_{ij} \cdot I_{DN} \cdot \cos \theta_{ij} \quad (1)$$

The direct normal solar radiation over the earth surface can be calculated as (Lee and Tavi, 2007):

$$I_{DN} = C_N \frac{A}{\exp(B/\sin \beta)} \quad (2)$$

where  $C_N$  is the clearness number from (McQuiston et al., 2000);  $A$  and  $B$  are solar coefficients from (ASHRAE, 1992).

For the cell that receives transmitted beam solar radiation passing through cell (p,q), the absorption of beam solar radiation can be calculated as follows:

$$I' = \alpha_{ij} \cdot (\tau_{pq} \cdot I_{DN} \cdot \cos \theta_{pq}) \cdot \cos \theta_{ij} \quad (3)$$

The incident angle for the cell (ij) of the dome surface can be calculated by

$$\cos \theta_{ij} = \frac{|-x_{ij} \cdot \cos \beta \cdot \cos \phi + y_{ij} \cdot \cos \beta \cdot \sin \phi - z_{ij} \cdot \sin \beta|}{R} \quad (4)$$

The diffuse solar radiation absorbed by the outside glazing surface is written as:

$$I_1'' = \alpha_{ij} \cdot (I_{ds,ij} + I_{dg,ij}) \quad (5)$$

The diffuse radiation heat flux from the sky can be calculated as follows:

$$I_{ds,ij} = C \cdot I_{DN} \cdot F_{ij,sky} \quad (6)$$

where  $C$  is solar coefficient from (ASHRAE, 1992).

The incident solar radiation on the ground is equivalent to the radiation flux on a horizontal surface and includes direct solar and diffuse sky radiation:

$$I_H = I_{DN}(C_1 + \sin \beta) \quad (7)$$

where  $C_1$  is coefficient from (ASHRAE, 1993).

From this, the ground reflected radiation may be calculated as:

$$I_{dg,ij} = I_H \gamma_g F_{ij,g,out} \quad (8)$$

The view factor from cell (ij) to the ground is written as follows:

$$F_{ij,g,out} = \frac{1 - \cos \Sigma_{ij}}{2} \quad (9)$$

The diffuse solar radiation absorbed by the inside cell surface is written as:

$$I_2'' = \alpha_{ij} \cdot \sum_{\substack{k=1,M \\ l=1,N}} F_{kl,ij} \cdot \tau_{kl} \cdot (I_{ds,kl} + I_{dg,kl}) \quad (10)$$

The total absorption of diffuse solar radiation is therefore written as:

$$I'' = I_1'' + I_2'' \quad (11)$$

The beam radiation transmitted through the cell reaching the exterior or wall surface is assumed to be absorbed by that wall surface. The area of each surface is assumed to be small enough so that the whole

radiation through that surface can be assumed to reach only one surface (wall, roof, or ground).

$$q_{sol,i,out} = \frac{\sum_{\substack{i=1,M \\ j=1,N}} \tau_{ij} \cdot A_{ij} \cdot \{I_{DN} \cdot \cos\theta_{ij} + F_{ij,l} \cdot (I_{ds} + I_{dg})\}}{A_i} \quad (12)$$

The ECG is able to allow the intake of valuable solar radiation into the dome structure while rejecting excessive heating. This can be done through different operation strategies, e.g., discrete strategy and continuous strategy.

Under discrete strategy, the ECG will fully darken to block 90% of the solar radiation to enter the inside of the dome upon receiving solar beam radiation over the glazing surface. Meanwhile, it will block 50% of the diffuse solar radiation (Porta-Gándara and Gómez-Muñoz, 2005). These changes are done through applying a direct current and varying its polarization voltage on the ECG. When maximum voltage of 5 V is applied, the glazing will fully darken and it remains clear when there is no voltage.

The overall transmittance of the cell under discrete strategy can be calculated by (Porta-Gándara and Gómez-Muñoz, 2005):

$$\tau_{ij} = (0.1 \cdot I_{beam,ij} + 0.5 \cdot I_{diff,ij}) / I_{total,ij} \quad (13)$$

When using continuous strategy, the darkening level is based on the incident beam radiation. The overall transmittance of the cell can then be calculated by (Porta-Gándara and Gómez-Muñoz, 2005):

$$\tau_{ij} = 0.4 \cdot (1 - I_{beam,ij} / I_{max}) + 0.1 \quad (14)$$

A variable direct current voltage, between 0 and 5 V, is applied to the ECG. The voltage is proportional to the solar radiation reaching the cell.

#### Thermal model for the glazing and the house

The dome is divided into a large number of cells and the heat balance equation for cell (i,j) can be written as:

$$k \cdot d \cdot l_{i+1,j} \cdot (T_{i+1,j} - T_{i,j}) + k \cdot d \cdot l_{i-1,j} \cdot (T_{i-1,j} - T_{i,j}) + k \cdot d \cdot l_{i,j-1} \cdot (T_{i,j-1} - T_{i,j}) + k \cdot d \cdot l_{i,j+1} \cdot (T_{i,j+1} - T_{i,j}) + (q_{sol,ij} + q_{conv,ij} + q_{LWR,ij} + q_{surf,ij}) \cdot A_{ij} = m_{ij} \cdot c_p \cdot \frac{dT}{dt} \quad (15)$$

For the heat balance inside the house, the following heat transfer processes are considered: the convection over the wall surfaces, the infiltration/exfiltration heat gain/loss to the house, heat gain from electrical appliances, people and heating system. The heat balance equation of the room air is written as:

$$Q_{HVAC} + \sum_{j=1}^9 A_j h_a (T_{j,in} - T_a) + Q_{exf} + Q_{internal,conv} = 0 \quad (16)$$

#### Air flow model inside the dome

Zonal model is developed to avoid substantial computational effort by CFD (Inard et al., 1996; Wurtz et al., 1999; Haghghat et al., 2001). The air space inside the dome is divided into a large number of zones, and the mass balance of each zone can be written as (Haghghat et al., 2001):

$$\sum_{i=1}^n \dot{m}_{ij} + \dot{m}_{source} + \dot{m}_{sink} = 0 \quad (17)$$

Under unsteady state, the energy balance for each zone can be written as:

$$\frac{dE_i}{dt} = \sum_{i=1}^n \dot{E}_{ij} + \dot{E}_{source} + \dot{E}_{sink} \quad (18)$$

#### Integrated thermal and airflow with house occupant behaviors model

Occupant behaviors can be physically modeled on the occupants' activities on window opening, shading, living habits, thermostat setpoint adjusting and light-switching habits, as well as electrical appliances usage pattern (Lin et al., 2015). The following section expressed the model on the usage of electrical appliances.

The operating energy need for the electrical appliances can be calculated as (Lin et al., 2015):

$$E_i = f_{n,i} \cdot AVG_i \quad (19)$$

AVG<sub>i</sub> is the average power input per cycle and can be calculated as the following (Lin et al., 2015):

$$AVG_i = \frac{\sum_{j=1}^N P_{i,j} \tau_j}{\sum_{j=1}^N \tau_j} \quad (\text{for one appliance}) \quad (20 - a)$$

$$AVG_i = \frac{\sum_{k=1}^M f_{d,k} \frac{\sum_{j=1}^N P_{k,j} \tau_j}{\sum_{j=1}^N \tau_j}}{\sum_{k=1}^M f_{d,k}} \quad (\text{for a group of appliances}) \quad (20 - b)$$

#### Numerical solution

This mathematical model involves linear and nonlinear equations. The nonlinear equations exist because of long-wave radiation and coupling of air movement and heat transfer. To solve this problem, the radiation coefficients are employed. The whole system of equations for temperature is considered as quasi-linear. The radiation coefficients are generated by using total interchange view factors and updated surface temperature during the calculation process. The system of equations thus is divided into two sub-systems—one containing the temperature and one containing the pressure differences and solved using the coupling approach. It can be written as follows:

$$\begin{bmatrix} \mathbf{A} & \mathbf{O} \\ \mathbf{O} & \mathbf{C} \end{bmatrix} \begin{bmatrix} \mathbf{T} \\ \mathbf{P} \end{bmatrix} = \begin{bmatrix} \mathbf{B} \\ \mathbf{D} \end{bmatrix} \quad (21)$$

Matrix A contains the thermal and optical properties. Matrix C contains the zone interface properties. Matrixes B and D represent the temperature and pressure driving forces.

The solution procedure can be summarized as follows (Fig. 2): (1) read the input data (weather data, geometric data and thermal properties) from the input file; (2) calculate the time independent coefficients for the program, including view factors between each cell and the wall surface, roof surface and ground surface and the areas for each part of the dome surface (these coefficients are for long-wave radiation), and calculate the total interchange view factor between all surfaces; The Gauss-Seidel iteration scheme is used to calculate the total interchange view factor. (3) calculate the incident solar radiation over each surface and the internal heat gain of the house for every time

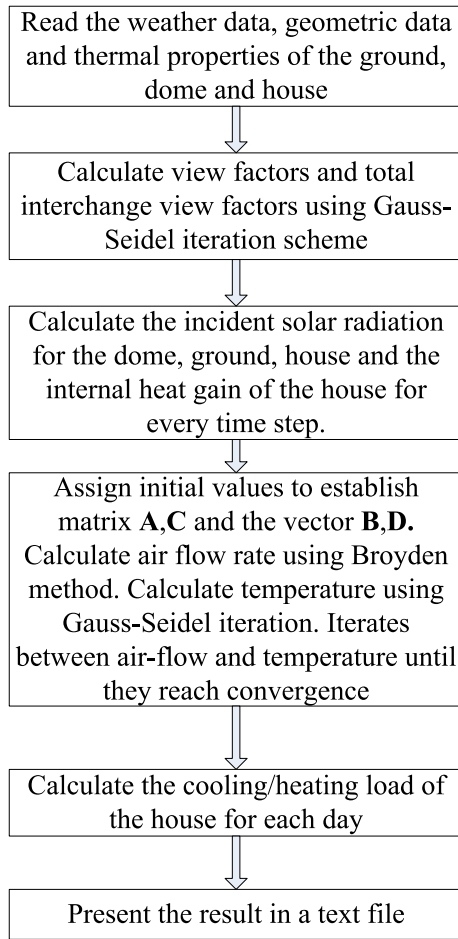


Fig. 2. Flow chart for the overall calculation procedure.

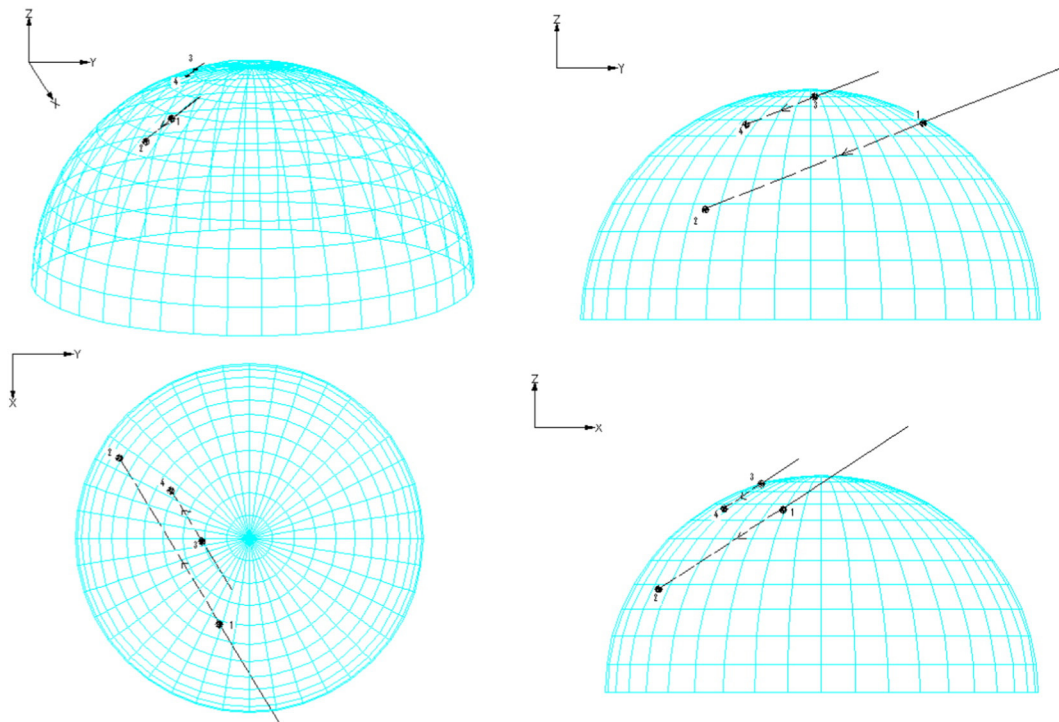


Fig. 3. Solar radiation from different view point.

Table 1  
Solar radiation.

No.	Item	Total (W)
	Total solar radiation coming into the dome	211,863.6
1	Total solar radiation reaching the ground	144,534.5
2	Total solar radiation reaching the west wall	257.5
3	Total solar radiation reaching the south wall	13,080.9
4	Total solar radiation reaching the east wall	6618.0
5	Total solar radiation reaching the north wall	253.8
6	Total solar radiation reaching the roof	15,400.3
7	Total beam solar radiation absorbed by the dome glazing or coming out from the dome glazing	26,034.1
8	Total diffuse solar radiation absorbed by the dome glazing or coming out from the dome glazing	5686.6
Total solar radiation absorbed and coming out from the dome (1–8)		211,865.7

step. (4) assign the initial temperature to each node, assign air pressure to each zone, compute for the air flow rate between adjacent zones, and establish the matrix **A** and the vector **B**, as well as matrix **C** and the vector **D**. The Broyden method is used to calculate the air flow rate, and the Gauss-Seidel iteration scheme is used for solving the system of equations for the temperature; Iterates between air-flow and temperature until they reach convergence; (5) Calculate the cooling/heating load of the house for each day; (6) present the result in a text file.

### Verification and validation

In this section, various ways of program verification and validation are presented. Firstly, the calculation of the direction of transmitted solar beam and solar energy balance are verified. Secondly, the program's response on a step input of the outside air temperature changes are tested by comparing with measured data for a small dome. Thirdly, the variation of inside air temperature is verified by comparing the results from a 2-D CFD model. The CFD model is solved using COMSOL Multiphysics (Smith, 1999). Finally, the results from the computer program are compared with measured data as well as simulation results from other researchers. Through the verification and validation,

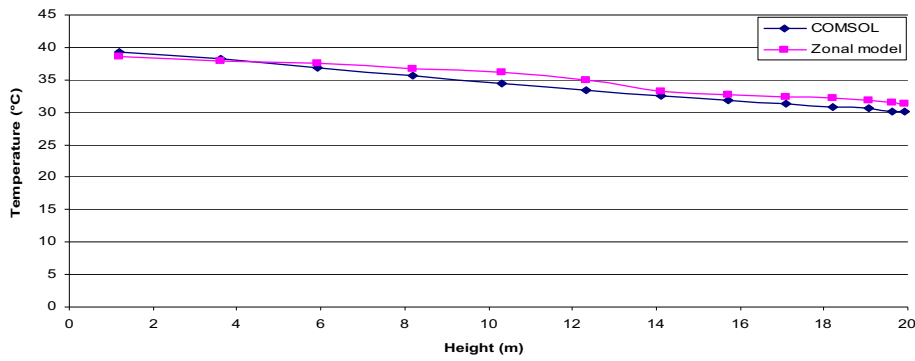


Fig. 4. Comparison between the computer model and the COMSOL program on the average inside air temperature.

it is proved that the model have good prediction on the temperature of the dome glazing, and the dome air temperature. Therefore, it can be used to predict the thermal environment inside the dome.

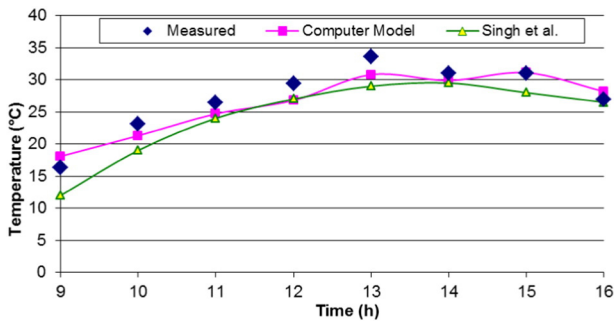
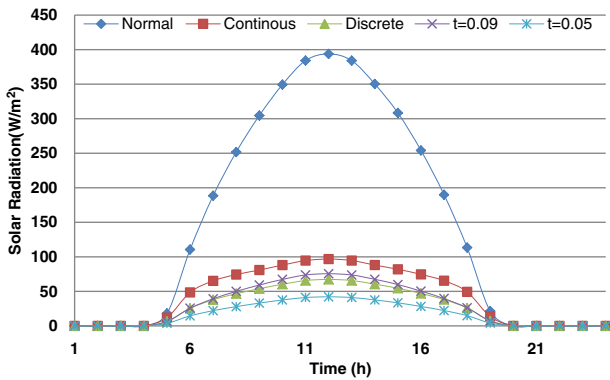


Fig. 5. Comparison between the inside air temperatures with simulation and measurements from Singh et al. (2006) on January 26th.

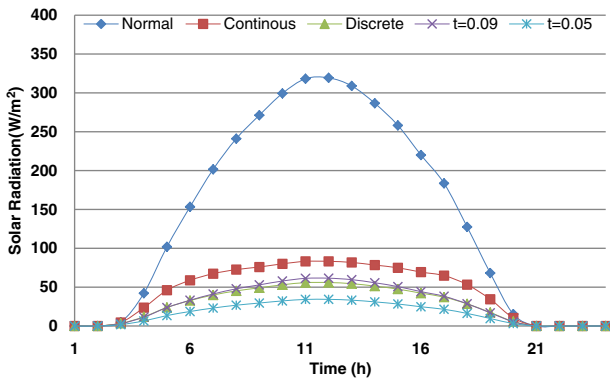
Verification on the calculation of solar beam and solar energy balance

The solar radiation transmitted through the dome (height = 13.15 m, base radius = 18.5 m) at 10:00 AM on January 21st, Montreal (solar azimuth = -31.2° from due south) is selected for the verification of solar energy balance and direction of solar beam. Fig. 3 shows some of the solar beam transmitted through the dome and reaches other side of the dome based on calculation. It is observed that the direction of the solar beam is about 31° from due south. Therefore, the computer calculation of the solar beam is valid.

Table 1 presents the balance of solar radiation. It is observed that the total amount of incident solar radiation on the dome glazing is equal to the total solar radiation absorbed by each surface and absorbed or coming out from the dome glazing. Therefore, the calculation of the solar energy by the computer program is valid.

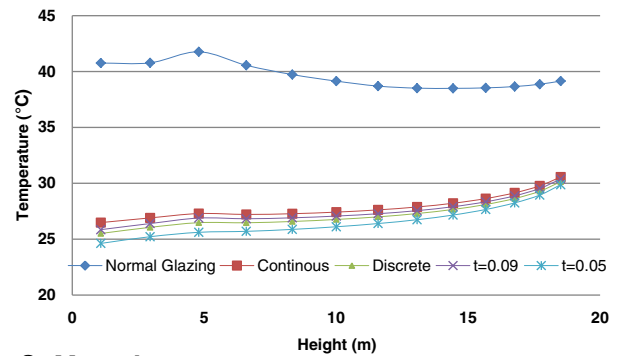


a. Montreal

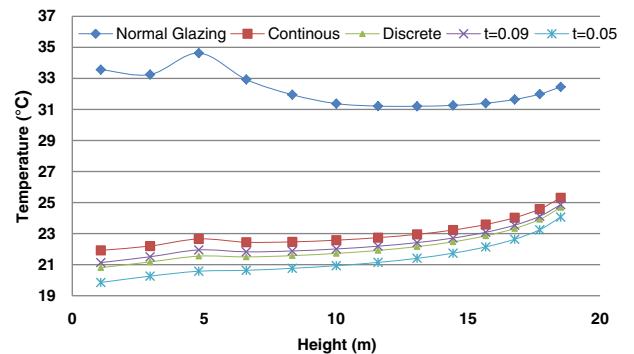


b. Yellowknife

Fig. 6. Solar Radiation Absorbed by the inside Ground Surface on July 21st.



a. Montreal



b. Yellowknife

Fig. 7. Variation of the inside Air Temperature with height at the core zone inside the dome at 13 PM on July 21st.

### Verification on the program's response on a step input

The response of the system on a step input is tested by comparing with experimental data for from (COMSOL AB, 2012) for two cases. In the first case, the temperature of the dome and of the inside air initially stays at 0 °C, and suddenly the outdoor air temperature rises to 19.25 °C. In the second case, the initial temperature of the dome and inside air is (−4.65 °C) and the outside air temperature rises to 22.85 °C. The simulation results agree well with experimental data on the glazing temperature with maximum temperature difference of less than 0.1 °C.

### Verification on the air temperature and air flow distributions with CFD model

A 2-D dimensionless CFD model is defined in the COMSOL Multiphysics environment (Smith, 1999) using the dome diameter as the characteristic length. The boundary conditions for the COMSOL Multiphysics model are: the temperature of the glazing (13 cells for the western part and 13 cells for the eastern part), and inside ground surface temperature. The results on the air temperature distribution, as predicted by the computer model, are compared with the ones predicted by the COMSOL Multiphysics program.

Fig. 4 present the difference between the average inside air temperature, as predicted by the computer model and the COMSOL program. The cover temperature above the height of 13.26 m is fixed at 30 °C,

and the ground temperature at 40 °C. The part of dome-cover with height below 13.26 m is well insulated. The maximum and difference between the average predicted air temperature by the computer model and the COMSOL program are 1.7 °C (4.8%), and 0.49 °C (1.4%), respectively. The air flow patterns predicted by the computer model and the COMSOL program are also quite similar. The computer model predictions are quite close with the COMSOL program.

### Verification and validation of the computer program by simulation and experimental measurements on a greenhouse

Comparison among the average inside air temperature predicted by the computer model and the experimental data and simulation results from (Singh et al., 2006), on January 26th, for a greenhouse located in India, is shown in Fig. 5. A dome with radius of 6 m, height of 3.5 m, normal transmittance of 0.65 and absorptance of 0.2, is used to represent the greenhouse in the computer model. The inside air temperature was measured at 32 points at four vertical cross-sections at 6 m difference along the length. The temperature of bare soil surface and solar radiations normal to earth surface were measured at single point.

The computer model predicts similar trend of variation of the indoor air temperature, as compared with average temperature from the measurements. The maximum and mean difference between the predictions by the computer model and measurements for the indoor air are 2.8 °C (8.3%) and 0.85 °C (3.2%), respectively. The simulation results

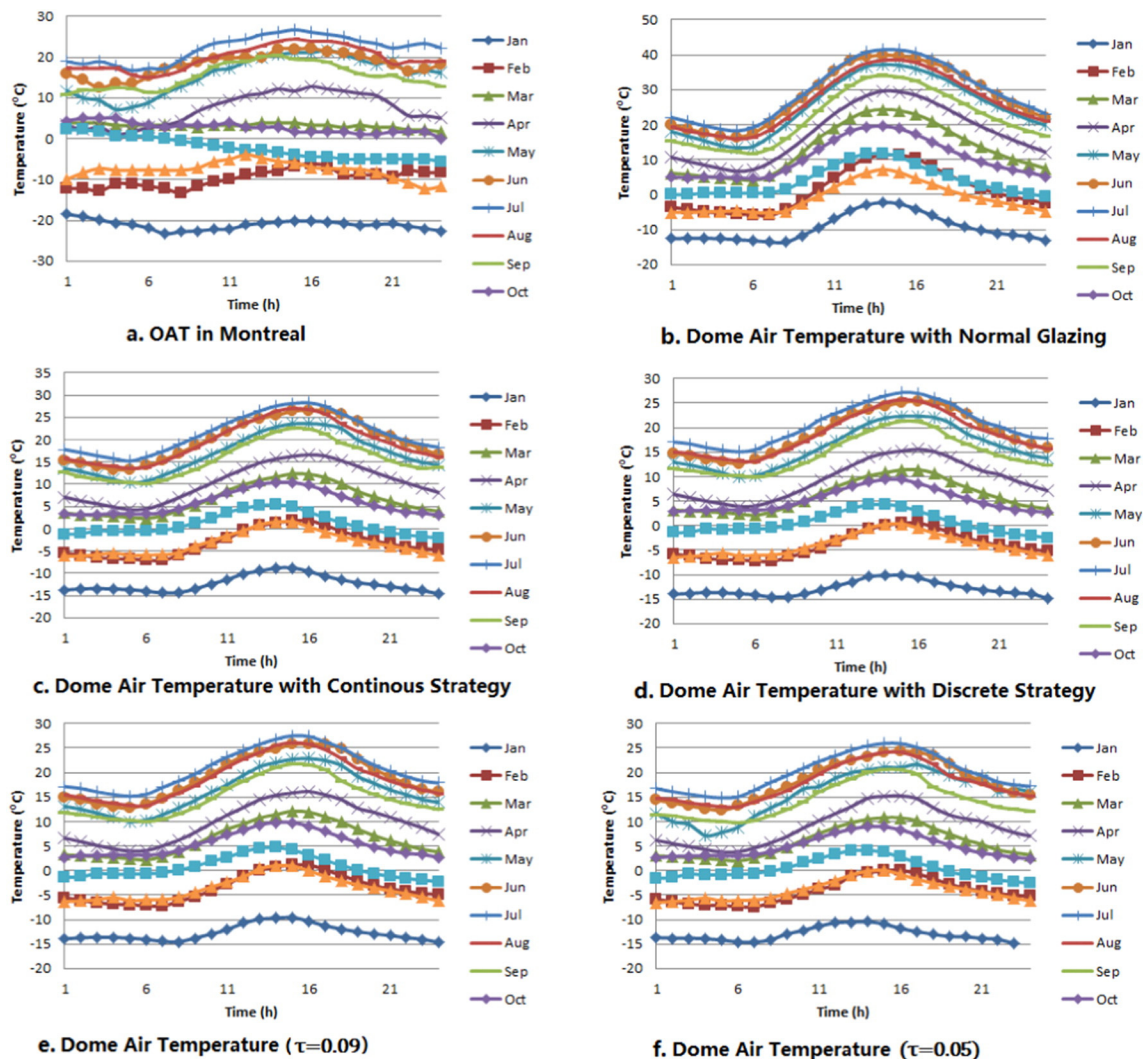


Fig. 8. Comparison on the inside dome air temperature in Montreal.

are considered as acceptable because: (1) the shapes in the computer model and greenhouse are not exactly the same; (2) the comparison is made based on the average temperature.

**Case studies**

A dome with the radius of 20 m, built around a house with 100 m<sup>2</sup> floor area and 4 m height, is used as a case for study. The weather data for one typical day per month, including ambient temperature, wind speed and direction, are from (Environment Canada, 2014). The thickness of the glazing is 24.4 mm. For the clear glazing, the normal transmissivity is 0.5 and reflectance is 0.06. The thermal resistance of the external walls of the house located in Montreal is 3.4 m<sup>2</sup> °C/W and for Yellowknife is 3.6 m<sup>2</sup> °C/W. For the unprotected house, the natural ventilation rate is 0.15 ACH. The window-to-wall ratio is 15%. The heating air temperature setpoint is held at 21 °C.

Fig. 6 presents the solar radiation absorbed by the inside ground surface. The reduction of absorption of solar radiation on July 21st in Montreal, as compared to the normal glazing, are 71.6%, 81.7%, 80.1% and 88.9% under continuous strategy, discrete strategy,  $\tau = 0.09$  and  $\tau = 0.05$ , respectively. For the case in Yellowknife, the reduction rates become 68.9%, 80.8%, 79.7% and 88.6%, which are slightly lower than the ones in Montreal. However, it is observed that significant reduction on the absorbed solar radiation can be achieved.

Fig. 7 presents the variation of the inside air temperature with height at the core zone inside the dome at 13 PM on July 21st in Montreal and Yellowknife respectively. The highest air temperature inside the dome at be as high as 41.8 °C in Montreal and 34.6 °C in Yellowknife if normal glazing is used. When electrochromic/low transmissivity glazing is used, it can be reduced to as low as 25.6 °C in Montreal and 20.6 °C in Yellowknife when the height is lower than 4 m.

Figs. 8 and 9 present the variation of the dome air temperature (the highest temperature among all the zones) in Montreal and Yellowknife, respectively. For the case in Montreal, there is a total of six months (from April to September) that the highest dome air temperature can reach 30 °C. For the case in Yellowknife, there are three months (June, July and August) that the total number of months that the highest dome air temperature can reach 30 °C. When electrochromic/low transmissivity glazing is used, this number can be reduced to 0.

Tables 2 and 3 compare the average heating load of the house during winter season. It can be seen that the use of dome glazing helps to achieve daily heating load reduction rates between 67.0% and 77.7% in Montreal. The use of normal glazing can help reduce almost 10% more in heating load as compared to electrochromic glazing. For the case in Yellowknife, the range of reduction rates is from 41.9% to 45.3%, and there is no big difference in the reduction of heating load between normal glazing and electrochromic glazing, which means that the reduction

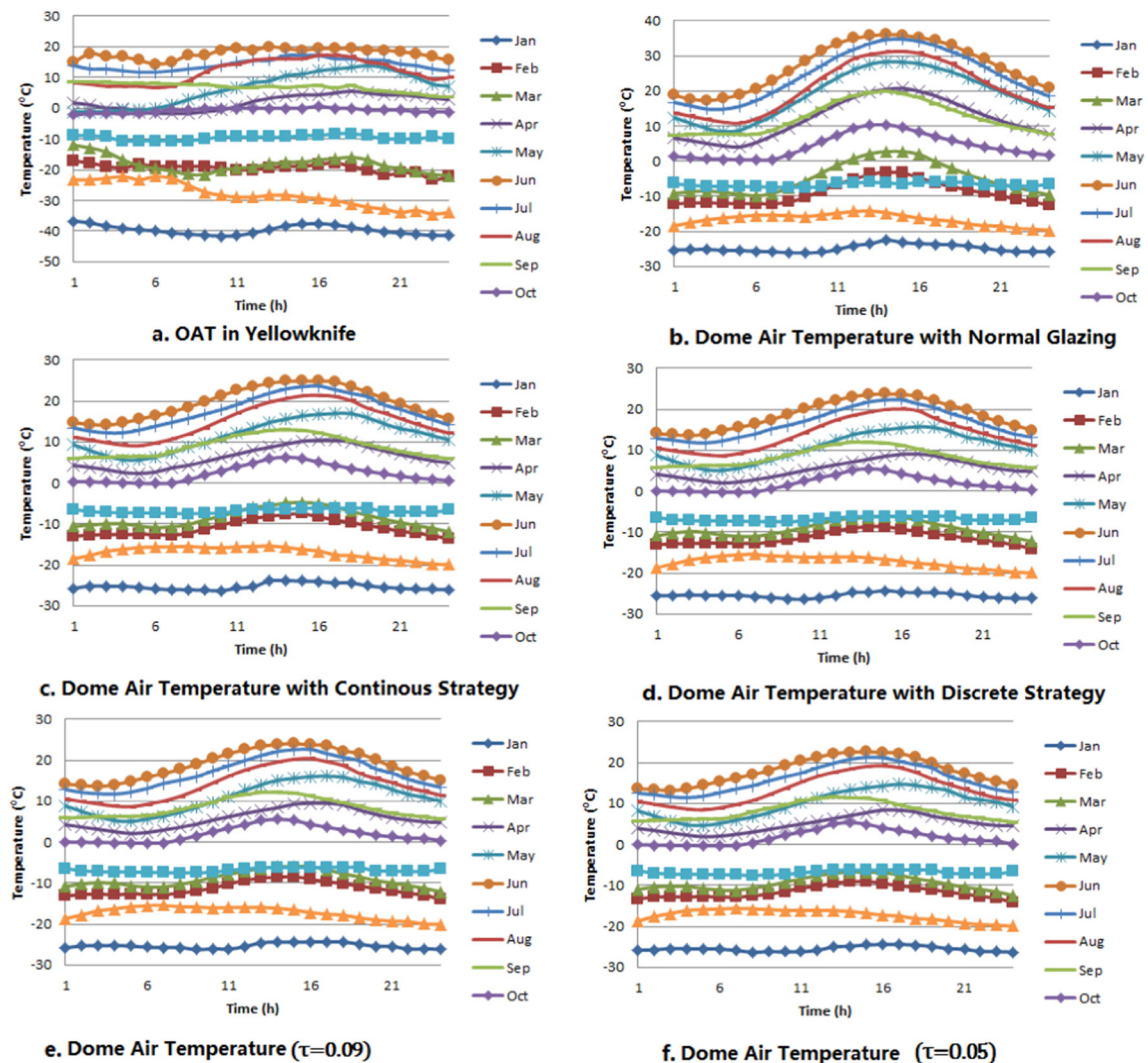


Fig. 9. Comparison on the inside dome air temperature in Yellowknife.

**Table 2**  
Average heating load of the house in Yellowknife, in kW.

	Average heating load Nov–Feb (kW)	Reduction rate(%)
Without dome	5.61	–
Normal	3.07	45.3%
Continuous	3.21	42.9%
Discrete	3.25	42.1%
$\tau = 0.09$	3.24	42.3%
$\tau = 0.05$	3.26	41.9%

**Table 3**  
Average heating load of the house in Montreal, in kW.

	Average heating load Nov–Feb(kW)	Reduction rate(%)
Without dome	4.55	–
Normal	1.02	77.7%
Continuous	1.41	68.9%
Discrete	1.48	67.5%
$\tau = 0.09$	1.45	68.2%
$\tau = 0.05$	1.50	67.0%

probably comes mostly from reduction on the wind speed in winter, thus significantly reducing the outside convection coefficients. Mechanical cooling is not required when electrochromic glazing is used. The house air temperature can be held at  $<28^{\circ}\text{C}$  in summer through natural ventilation with dome and  $<29^{\circ}\text{C}$  for a normal house in Montreal. If mechanical cooling is used to maintain the house air temperature at  $26^{\circ}\text{C}$ , a reduction rate of 26.8% in cooling load can be achieved as compared with a normal house, which is due to lower ambient air temperature and ground temperature.

## Conclusions

The use of dome-glazing can reduce the house heating energy need under cold climate. However, in summer time, the dome becomes a green-house, and therefore, the dome air temperature can be increased to a level that makes it no longer suitable to live in without air-conditioning. Electrochromic glazing can help to prevent the solar radiation from entering the dome when the radiation intensity is high, so the air temperature inside the dome can be much lower than the one with normal glazing because of less absorption on solar radiation and thus can create a comfortable thermal environment. It is also worth mentioning that there is no great difference on the variation of dome air temperature and heating load of the house under different control strategies for electrochromic glazing. For the case in Yellowknife, low transmissivity glazing can be used to replace electrochromic glazing to achieve similar results in reduction of the heating load as well as maintaining low air temperature inside the dome in summer.

## Acknowledgement

The authors acknowledge the financial support from Natural Sciences and Engineering Research Council of Canada and the overseas PhD funding from Wuhan University of Technology.

## References

- Aldawoud A. Conventional fixed shading devices in comparison to an electrochromic glazing system in hot, dry climate. *Energy Buildings* 2013;59:104–10.
- Arslan S, Sorguc AG. Similarities between “structures in nature” and “man-made structures”: biomimesis in architecture. In: Collins MW, Brebia CA, editors. *Design and nature II*. WIT Press; 2004. p. 45–54.
- ASHRAE. Cooling and heating load calculation manual. 2nd ed. Atlanta, USA: American Society of Heating, Refrigerating, and Air-Conditioning Engineers; 1992.
- ASHRAE. *ASHRAE Handbook Fundamentals*, Chapter 3. Atlanta, USA: American Society of Heating, Refrigerating, and Air-Conditioning Engineers; 1993.
- COMSOL AB. COMSOL multiphysics user's guide. MA, USA: Burlington; 2012.
- Croome DJ, Moseley P. Energy and thermal performance of airhouses. *Proceedings of the design of air-supported structures*. Bath, UK: University of Bath; 1984. p. 223–37.
- EnergyPlus, [http://apps1.eere.energy.gov/buildings/energyplus/?utm\\_source=EnergyPlus&utm\\_medium=redirect&utm\\_campaign=EnergyPlus%2Bredirect%2B1](http://apps1.eere.energy.gov/buildings/energyplus/?utm_source=EnergyPlus&utm_medium=redirect&utm_campaign=EnergyPlus%2Bredirect%2B1), (Last Time Accessed: July) 2016.
- Environment Canada. [http://www.climate.weatheroffice.ec.gc.ca/climateData/canada\\_e.html](http://www.climate.weatheroffice.ec.gc.ca/climateData/canada_e.html), 2014. (Accessed on 15 July 2014).
- eQuest, <http://www.doe2.com/equest/>, (Last Time Accessed: July) 2016.
- ESP-r, <http://www.esru.strath.ac.uk/Programs/ESP-r.htm>, (Last Time Accessed: July) 2016.
- Haghighat F, Lin Y, Megri AC. Development and validation of a zonal model—POMA. *Build Environ* 2001;36(9):1039–47.
- Inard C, Bouia H, Dalicieux P. Prediction of air temperature distribution in buildings with a zonal model. *Energy Build* 1996;24(2):125–32.
- Lee ES, DiBartolomeo DL. Application issues for large-area electrochromic windows in commercial buildings. *Sol Energy Mater Sol Cells* 2002;71:465–91.
- Lee ES, Tavil A. Energy and visual comfort performance of electrochromic windows with overhangs. *Build Environ* 2007;42:2439–49.
- Lee ES, Claybaugh ES, LaFrance M. End user impacts of automated electrochromic windows in a pilot retrofit application. *Energy Buildings* 2012;47:267–84.
- Lin Y. Three-dimensional thermal and airflow (3D-TAF) model of a dome-covered house in Canada. Ph. D. Thesis Concordia University: Department of Building, Civil and Environmental Engineering; 2007.
- Lin Y, Yang W, Gabriel KS. A study on the impact of household occupants' behavior on energy consumption using an integrated computer model. *Front Built Environ* 2015;1:16. <http://dx.doi.org/10.3389/fbuil.2015.00016>.
- Luttmann-Valencia F. A dynamic thermal model of a self-sustaining closed environment life support system (Ph.D. Dissertation) Tucson: University of Arizona; 1990.
- McQuiston FC, Parker JD, Spitler JD. *Heating, ventilating, and air conditioning: analysis and design*. New York, USA: John Wiley & Sons; 2000.
- Piccolo A, Simone F. Effect of switchable glazing on discomfort glare from windows. *Build Environ* 2009;44:1171–80.
- Pittaluga M. The electrochromic wall. *Energy Buildings* 2013;66:49–56.
- Porta-Gándara MA, Gómez-Muñoz V. Solar performance of an electrochromic geodesic dome roof. *Energy* 2005;30(13):2474–86.
- Sbar NL, Podbelski L, Yang HM, Pease B. Electrochromic dynamic windows for office buildings. *Int J Sustain Built Environ* 2012;1:125–39.
- Sharma PK, Tiwari GN, Sorayan VPS. Temperature distribution in different zones of the micro-climate of a greenhouse: a dynamic model. *Energy Convers Manage* 1999;40(3):335–48.
- Singh G, Singh PP, Lubana PPS, Singh KG. Formulation and validation of a mathematical model of the microclimate of a greenhouse. *Renew Energy* 2006;31(10):1541–60.
- Smith AM. Prediction and measurement of thermal exchanges within pyranometers (MS Thesis) Virginia, USA: Virginia Polytechnic Institute; 1999.
- Stach E. Form-optimizing processes in biological structures-self-generating structures in nature based on pneumatics. In: Collins MW, Brebia CA, editors. *Design and nature II*. WIT Press; 2004. p. 3–14.
- TRNSYS, <http://sel.me.wisc.edu/trnsys/>, (Last Time Accessed: July) 2016.
- Tsui E. *Evolutionary architecture*. New York, USA: John Wiley; 1999.
- Wurtz E, Nataf JM, Winkelmann F. Two- and three-dimensional natural and mixed convection simulation using modular zonal models in buildings. *Int J Heat Mass Transf* 1999;42(5):923–40.